The time-dependent extrudate-swell problem of an Oldroyd-B fluid with slip along the wall

Eric Brasseur

Unité de Mécanique Appliquée, Université Catholique de Louvain, Bâtiment Euler, 4–6 Avenue Georges Lemaitre, B-1348 Louvain-la-Neuve, Belgium

Marios M. Fyrillas and Georgios C. Georgiou[a)]

Department of Mathematics and Statistics, University of Cyprus, Kallipoleos 75, P.O. Box 537, CY-1678 Nicosia, Cyprus

Marcel J. Crochet

Unité de Mécanique Appliquée, Université Catholique de Louvain, Bâtiment Euler, 4–6 Avenue Georges Lemaitre, B-1348 Louvain-la-Neuve, Belgium

(Received 17 September 1997; final revision received 6 January 1998)

Synopsis

We demonstrate that viscoelasticity combined with nonlinear slip acts as a storage of elastic energy generating oscillations of the pressure drop similar to those observed experimentally in extrusion instabilities. We consider the time-dependent axisymmetric incompressible Poiseuille and extrudate-swell flows of an Oldroyd-B fluid. We assume that slip occurs along the wall of the die following a slip equation which relates the shear stress to the velocity at the wall and exhibits a maximum and a minimum. We first study the stability of the one-dimensional axisymmetric Poiseuille flow by means of a one-dimensional linear stability analysis and time-dependent calculations. The numerically predicted instability regimes agree well with the linear stability ones. The calculations reveal that periodic solutions are obtained when an unstable steady-state is perturbed and that the amplitude and the period of the oscillations are increasing functions of the Weissenberg number. We then continue to numerically solve the time-dependent two-dimensional axisymmetric Poiseuille and extrudate-swell flows using the elastic-viscous split stress method for the integration of the constitutive equation. Again, oscillations are observed in the unstable regime; consequently, the surface of the extrudate is wavy. However, the amplitude and the period of the pressure drop oscillations are considerably smaller than in the one-dimensional flow. The most important phenomenon revealed by our two-dimensional calculations is that the flow in the die is periodic in the axial direction. © *1998 The Society of Rheology.* [S0148-6055(98)00103-5]

I. INTRODUCTION

Two basic explanations for the stick-slip and the gross fracture instabilities, observed during the extrusion of polymeric fluids from a capillary or a slit, are the loss of adhesion at the polymer-wall interface and the constitutive instabilities. Most slip equations proposed in the literature predict a power-law relation between the shear stress at the wall and the slip velocity (at constant temperature) [Denn (1992)]. Of particular interest to this

[a)]Author to whom correspondence should be addressed.

work, however, are equations which exhibit maxima and minima. If such a slip equation holds, the corresponding flow curve for Poiseuille flow, i.e., the log–log plot of the pressure drop versus the flow rate (or, equivalently, the log–log plot of the wall shear stress versus the apparent shear rate), exhibits maxima and minima too. Non-monotone slip equations based on molecular parameters have been proposed by El Kissi and Piau (1989), by Leonov (1990) and by Adewale and Leonov (1997).

Pearson and Petrie (1965) carried out the linear stability analysis of the incompressible Newtonian Poiseuille flow with slip at the wall for two-dimensional disturbances showing that the flow is linearly unstable when the slope of the slip function is negative. Georgiou and Crochet (1994a) numerically solved the time-dependent compressible Newtonian Poiseuille flow with nonlinear slip at the wall, showing that, indeed, steady-state solutions in the negative-slope regime of the flow curve are unstable. If such a solution is perturbed, self-sustained oscillations of the pressure drop and of the mass flow rate at the exit are obtained, while the volumetric flow rate at the inlet is kept constant. These oscillations are similar to those observed with the stick-slip instability. The calculations have been extended to the extrudate-swell problem [Georgiou and Crochet (1994b)], and, as expected, the surface of the extrudate is oscillatory in the unstable regime. The amplitude and the wavelength of the free-surface waves increase with compressibility.

While the above mechanism of slip-induced instability is based on the multi-valuedness of the slip equation, most of the proposed studies of constitutive instability are caused by the multi-valuedness of the constitutive equation, i.e., at a given shear stress there are three different shear rates that correspond. Linear stability and/or time-dependent numerical analyses of the shear and Poiseuille flows of fluids obeying non-monotone constitutive equations show that steady-state solutions in the negative-slope regime of the constitutive equation may be unstable and that a flow curve hysteresis is obtained between the two stable branches [Yerushalmi (1970); Kolkka *et al.* (1988)]. Interesting discussions and comparisons between the wall slip and the constitutive instabilities mechanisms can be found in Chen *et al.* (1994) and Adewale and Leonov (1997).

In our previous work [Georgiou and Crochet (1994a,b)], we have shown that compressibility in combination with nonlinear slip at the wall acts as a storage of elastic energy generating oscillations of the pressure drop and of the mass flow rate in Poiseuille flow. The objective of the present work is to demonstrate that viscoelasticity combined with nonlinear slip plays a similar role in incompressible viscoelastic flow. For this purpose, we use the Oldroyd-B model which exhibits a monotonic steady-shear response. The proposed mechanism of instability does not require any multi-valuedness of the constitutive equation; the multi-valuedness of the flow curve is solely due to the slip equation.

We solve the time-dependent axisymmetric extrudate-swell problem of an Oldroyd-B fluid; we also present results for the one- and two-dimensional axisymmetric Poiseuille and the stick-slip problems. The governing equations and the boundary conditions are presented in Section II. For the integration of the constitutive equation we use the elastic-viscous split stress (EVSS) method of Rajagopalan *et al.* (1990) which has shown convergence at high values of elasticity at relatively low computational cost. For solving this time-dependent free-surface viscoelastic flow problem, we use the finite element method with a second-order predictor–corrector scheme for integration in time. The numerical method is described briefly in Section III. Before proceeding to the solution of the two-dimensional problems, we study the stability of the one-dimensional axisymmetric Poiseuille flow. In Section IV, we present the linear stability diagrams for one-dimensional infinitesimal disturbances showing that a steady-state solution in the

negative-slope regime of the flow curve might be unstable. Steady-state solutions in the negative-slope regime destabilize as we move from the Newtonian to the upper-convected Maxwell model or as elasticity increases. In Section V, we numerically solve the one-dimensional Poiseuille flow. The predicted instability regimes agree well with those of the linear stability analysis. If the imposed volumetric flow rate falls into the unstable regime, then the flow becomes periodic. The amplitude and the period of the pressure-drop oscillations increase with elasticity. Similar results have been obtained for the shear flow with slip along the fixed wall and are presented elsewhere [Georgiou (1996); Fyrillas and Georgiou (1997)]. Finally, in Section VI, we present numerical results for the two-dimensional axisymmetric Poiseuille, stick-slip, and extrudate-swell flows obtained with the EVSS method. Again, periodic solutions are generated when the imposed volumetric flow rate is in the unstable regime. However, the oscillations are of smaller amplitude and period than in the one-dimensional flow. Our calculations reveal that the flow in the die is space periodic and the surface of the extrudate exhibits small-amplitude waves.

II. GOVERNING EQUATIONS

Since the instabilities of interest originate in the die, we will first study the time-dependent Poiseuille flow before proceeding to the extrudate-swell problem. Furthermore, because the outflow conditions in time-dependent viscoelastic simulations may have a dramatic effect on the numerical solution [Bodart and Crochet (1993)], we will also consider the stick-slip flow problem. If $\mathbf{v}$ and σ are the velocity vector and the stress tensor, respectively, the continuity and the momentum equations for time-dependent incompressible flow may be written as follows:

$$\nabla\cdot\mathbf{v} = 0, \tag{1}$$

$$\rho\frac{\partial\mathbf{v}}{\partial t}+\rho\mathbf{v}\cdot\nabla\mathbf{v}-\nabla\cdot\boldsymbol{\sigma}-\mathbf{f} = \mathbf{0}, \tag{2}$$

where ρ is the density and $\mathbf{f}$ is the body force. The stress tensor $\boldsymbol{\sigma}$ can be written as

$$\boldsymbol{\sigma} = -p\mathbf{I}+\mathbf{T}, \tag{3}$$

where p denotes the pressure, $\mathbf{I}$ is the unit tensor and $\mathbf{T}$ is the extra-stress tensor.

We consider the Oldroyd-B constitutive model. The extra-stress tensor $\mathbf{T}$ is decomposed into a purely viscoelastic part $\mathbf{T_1}$ and a purely viscous part $\mathbf{T_2}$ [Crochet *et al.* (1984)]:

$$\mathbf{T} = \mathbf{T_1}+\mathbf{T_2}, \tag{4}$$

$$\mathbf{T_1}+\lambda\overset{\triangledown}{\mathbf{T}}_{\mathbf{1}} = 2\eta_1\mathbf{d}, \tag{5}$$

$$\mathbf{T_2} = 2\eta_2\mathbf{d}, \tag{6}$$

where η_1, η_2 and λ are material parameters. The Newtonian and the upper-convected Maxwell models are recovered by setting $\eta_1 = 0$ and $\eta_2 = 0$, respectively. Moreover, $\mathbf{d}$ is the rate-of-strain tensor defined by:

$$\mathbf{d} = \tfrac{1}{2}[(\nabla\mathbf{v})+(\nabla\mathbf{v})^T], \tag{7}$$

where the superscript T denotes the transpose. Finally, $\overset{\triangledown}{\mathbf{T_1}}$ is the upper-convected derivative of $\mathbf{T_1}$:

$$\overset{\triangledown}{\mathbf{T_1}} = \frac{D\mathbf{T_1}}{Dt} - (\nabla \mathbf{v})^T \cdot \mathbf{T_1} - \mathbf{T_1} \cdot \nabla \mathbf{v}. \tag{8}$$

We nondimensionalize the governing equations by scaling the lengths by the radius R of the die, the velocity by a characteristic velocity V, the stress components by $(\eta_1 + \eta_2)V/R$, and the time by R/V. We thus obtain two dimensionless numbers, the Reynolds number Re and the Weissenberg number We, defined as follows:

$$\mathrm{Re} \equiv \frac{\rho V R}{\eta_1 + \eta_2}; \quad \mathrm{We} \equiv \frac{\lambda V}{R}. \tag{9}$$

Equations (2) and (5) become:

$$\mathrm{Re}\frac{\partial \mathbf{v}}{\partial t} + \mathrm{Re}\mathbf{v} \cdot \nabla \mathbf{v} + \nabla p - \nabla \cdot (\mathbf{T_1} + \mathbf{T_2}) = \mathbf{0}, \tag{10}$$

$$\mathbf{T_1} + \mathrm{We}\,\overset{\triangledown}{\mathbf{T_1}} = 2\eta_1 \mathbf{d}. \tag{11}$$

Note that all the variables in the above two equations are dimensionless (η_1 and η_2 are scaled by the shear viscosity $\eta_1 + \eta_2$) and that the body force in the momentum equation has been neglected.

A. The elastic-viscous split stress formulation

We use the elastic-viscous split stress (EVSS) formulation for the integration of the constitutive equation [Rajagopalan *et al.* (1990)]. This method was especially developed for fluids with a Newtonian viscosity like the Oldroyd-B model but it also applies for fluids with an instantaneous elastic response like the UCM model. It is characterized by a bigger domain of convergence in We than other previous methods of comparable computational cost [Brown *et al.* (1993)]. The rate of deformation tensor $\mathbf{d}$, given by Equation (7), is introduced as an additional unknown along with the modified stress tensor $\mathbf{S}$ defined as follows:

$$\mathbf{S} = \mathbf{T_1} - 2\eta_1 \mathbf{d}. \tag{12}$$

Substituting into Equations (10) and (11) gives:

$$\mathrm{Re}\frac{\partial \mathbf{v}}{\partial t} + \mathrm{Re}\mathbf{v} \cdot \nabla \mathbf{v} + \nabla p - \nabla \cdot \mathbf{S} - 2\nabla^2 \mathbf{v} = \mathbf{0}, \tag{13}$$

$$\mathbf{S} + \mathrm{We}\left[\overset{\triangledown}{\mathbf{S}} + 2\eta_1 \overset{\triangledown}{\mathbf{d}}\right] = \mathbf{0}. \tag{14}$$

With the EVSS formulation the momentum/continuity equation set forms an elliptic saddle-point problem for the velocity and the pressure fields, if $\mathbf{T_1}$ is viewed as data for the equation set [Brown *et al.* (1993)].

B. Boundary and initial conditions

The geometry and the boundary conditions for the three time-dependent flows studied in this work are shown in Figure 1. We assume that slip occurs along the wall of the die following the slip equation used by Georgiou and Crochet (1994a). This equation relates the shear stress on the wall σ_w to the relative velocity of the fluid with respect to the wall v_w and involves three material parameters α_1, α_2 and α_3. Its nondimensionalized form is:

$$\sigma_w = -F(v_w) = -A_1\left(1+\frac{A_2}{1+A_3 v_w^2}\right)v_w, \tag{15}$$

where

$$A_1 \equiv \frac{\alpha_1 R}{\eta_1+\eta_2}; \quad A_2 \equiv \alpha_2; \quad A_3 \equiv \alpha_3 V^2. \tag{16}$$

Equation (15) exhibits a maximum and a minimum of σ_w provided that $A_2 > 8$; otherwise, the slip equation is monotonic. Another constraint arises if we demand that the volumetric flow rate Q for fully developed Poiseuille flow is a monotonic function of v_w. This requirement is met when

$$F'(v_w) > -4 \Leftrightarrow A_2 < 8\,\frac{4+A_1}{A_1}. \tag{17}$$

In Figure 2, we show the shear stress at the wall σ_w and the volumetric flow rate Q for fully developed Poiseuille flow as functions of v_w, for $A_1 = 1$, $A_2 = 20$ and $A_3 = 100$.

Along the axis of symmetry we have the usual symmetry conditions. Along the wall, the radial velocity vanishes whereas the axial velocity satisfies Equation (15). On the free surface we neglect surface tension and thus the normal and tangential stress components vanish. Another condition at the free surface is the kinematic one,

$$\frac{\partial h}{\partial t}+v_z\frac{\partial h}{\partial z}-v_r = 0, \tag{18}$$

which provides the additional equation required for the calculation of the unknown position of the free surface $h(z,t)$.

At the inlet plane, we impose the velocity components and all the components of the modified stress tensor **S**. In order to study the effect of the inlet boundary condition on the numerical solutions, we consider two possibilities. In the first case, v_z is assumed to be parabolic corresponding to the fully developed Poiseuille flow with slip along the wall:

$$\begin{gathered} v_z = v_z(r,v_w^I,Q) = (2r^2-1)v_w^I+2(1-r^2)Q; \quad v_r = S_{rz} = S_{rr} = S_{\theta\theta} = 0; \\ S_{zz} = 32\,\eta_1 \mathrm{We}\; r^2(v_w^I-Q)^2. \end{gathered} \tag{19}$$

Here v_w^I is the velocity at the wall calculated by demanding that v_z satisfies the slip Equation (15):

$$4(v_w^I-Q) = -A_1\left(1+\frac{A_2}{1+A_3(v_w^I)^2}\right)v_w^I. \tag{20}$$

In the second case, v_z is assumed to be uniform corresponding to plug flow:

$$v_z = Q; \quad v_r = S_{zz} = S_{rz} = S_{rr} = S_{\theta\theta} = 0. \tag{21}$$

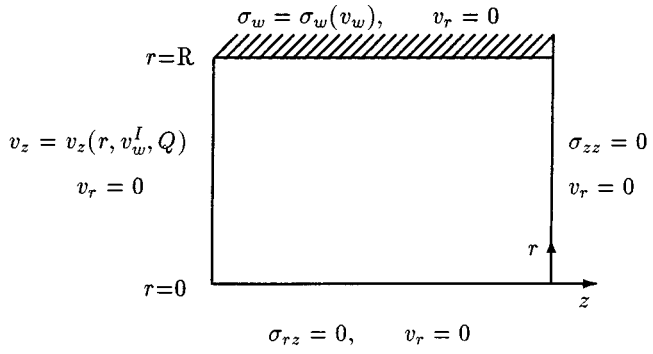

(a) Poiseuille flow

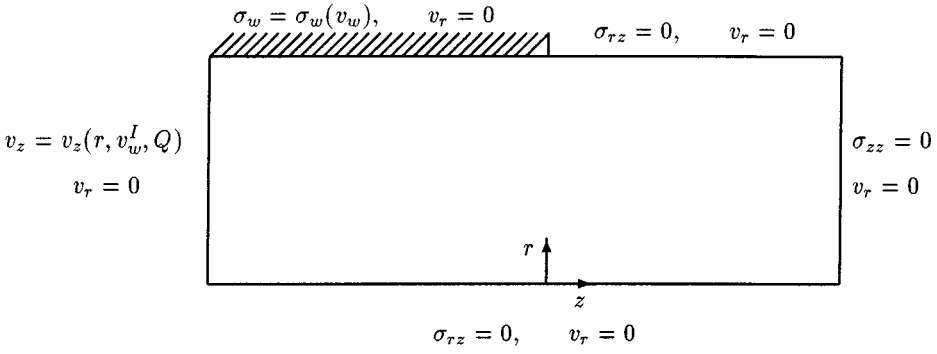

(b) Stick-slip flow

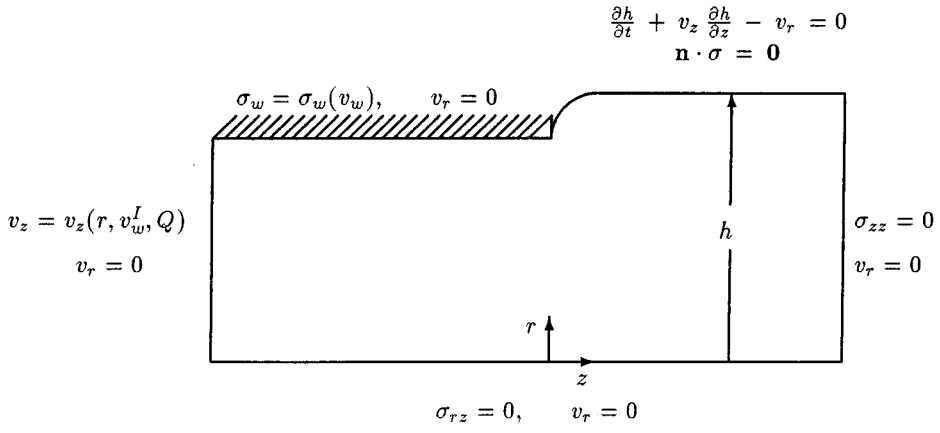

(c) Extrudate-swell flow

FIG. 1. Geometry and boundary conditions for the three time-dependent problems studied in this work; slip occurs along the wall.

(Note that Q is the dimensionless volumetric flow rate divided by π.) Finally, at the exit we assume that the radial velocity v_r and the normal stress σ_{zz} vanish. Note that σ_{zz} is not zero in the fully developed Poiseuille flow and hence our assumption makes the problem two dimensional.

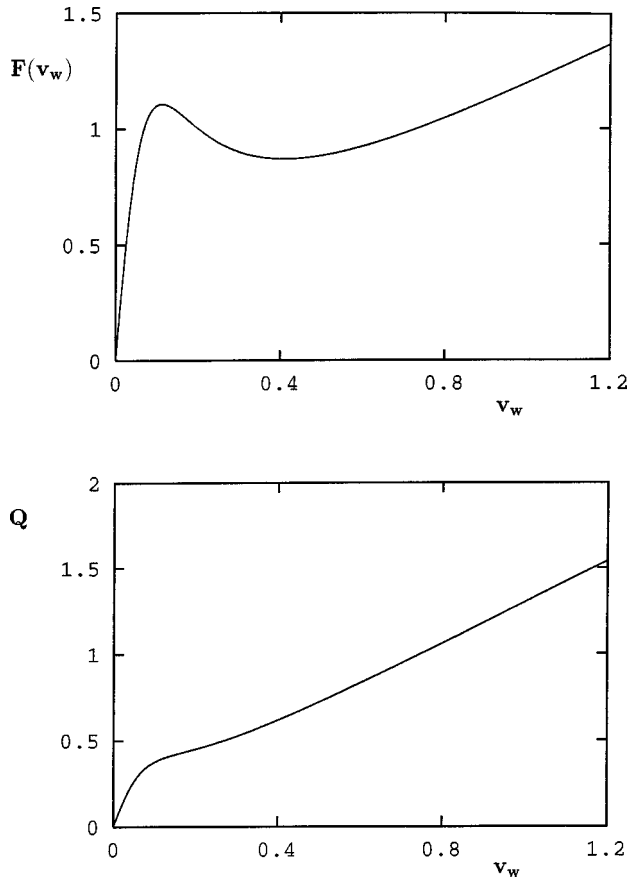

FIG. 2. Slip function and volumetric flow rate as functions of the slip velocity v_w; fully developed Poiseuille flow, $A_1 = 1$, $A_2 = 20$ and $A_3 = 100$.

As for the initial conditions, we start from the steady-state solution at a given volumetric flow rate Q_0 and we set $Q = Q_0 + \Delta Q$ at $t = \Delta t$. The values of v_z and S_{zz} at the inlet are then calculated using Equations (19) or (21).

III. FINITE ELEMENT FORMULATION

The full Newton iteration method is employed for solving the extrudate-swell problem. In other words, the unknown position of the free surface h is calculated simultaneously with the other fields. The two-dimensional spine remeshing technique is used at every Newton iteration step. An important issue in mixed finite element methods is the compatibility of the approximations used for the different unknown fields [see, for example, Brown *et al.* (1993)]. In the present work, we employ a P^2-C^0 (biquadratic) interpolation for the velocity vector and a P^1-C^0 (bilinear) interpolation for the pressure, the rate of deformation tensor and the modified stress tensor. For the position of the free surface we use a P^2-C^0 (quadratic) interpolation. Debae *et al.* (1994) have tested the EVSS method with the above set of approximations on different benchmark problems and found that it is remarkably stable and accurate despite its low cost. If the mesh, however, is of moderate refinement the method gives a slightly lower swelling than other more accurate methods.

The spatial discretization of the governing equations is performed via the Galerkin method. The resulting nonlinear system of equations is solved using the Newton method and a frontal solver. For time-dependent flow, we use a second-order predictor–corrector scheme. For the predictor we employ the explicit two-step Adams–Bashforth method while for the corrector we use the implicit Crank–Nicolson scheme. One iteration is allowed per time step. In the simple cases of Poiseuille flow, however, we also use the standard fully implicit (Euler backward-difference) scheme.

IV. THE ONE-DIMENSIONAL FLOW IN A TUBE

In the case of steady one-dimensional Poiseuille flow, it is easily shown that

$$v_z = v_w - \tfrac{1}{4}\nabla P(1-r^2), \tag{22}$$

$$T^{rz} = T_1^{rz} + T_2^{rz} = \nabla P \frac{r}{2}, \tag{23}$$

where the slip velocity v_w satisfies the condition

$$\sigma_w = \tfrac{1}{2}\nabla P = -F(v_w), \tag{24}$$

and ∇P is the pressure gradient. If Q is the volumetric flow rate divided by π,

$$Q = 2\int_0^1 v_z\, r\, dr, \tag{25}$$

then

$$Q = v_w - \tfrac{1}{8}\nabla P = v_w + \tfrac{1}{4}F(v_w). \tag{26}$$

As already mentioned, the Oldroyd-B model is a monotonic constitutive equation. It is easily deduced from Equations (24) and (26) that the shape of the flow curve is dictated by the slip equation (it exhibits a maximum and a minimum if the slip equation does).

A very useful result for the pressure gradient in time-dependent flow is obtained by integrating the z-momentum equation over the cross section of the die. If the volumetric flow rate is fixed, the left-hand side of the integrated equation is zero and we thus obtain:

$$-\nabla P = -2(T_1^{rz} + T_2^{rz})\big|_{r=1} = 2F(v_w). \tag{27}$$

The dependence of the pressure gradient ∇P on the slip velocity v_w is the same as in steady-state flow.

The stability of the steady-state solutions to one-dimensional infinitesimal disturbances can be studied by means of a linear stability analysis similar to that carried out by Fyrillas and Georgiou (1997) for the case of simple shear flow. In Poiseuille flow, either the volumetric flow rate or the pressure gradient can be fixed in time-dependent calculations. The neutral stability curves calculated with fixed volumetric flow rate are plotted in Figure 3 for various values of η_2. It can be shown that the stability curves of Figure 3 approach asymptotically the value $4\,\eta_2$.

As illustrated in Figure 3, for a given η_2, the stability of a basic solution is determined from the values of the derivative $F'(\bar{v}_w)$ and the elasticity number ε, defined as follows:

$$\varepsilon \equiv \frac{\mathrm{We}}{\mathrm{Re}}. \tag{28}$$

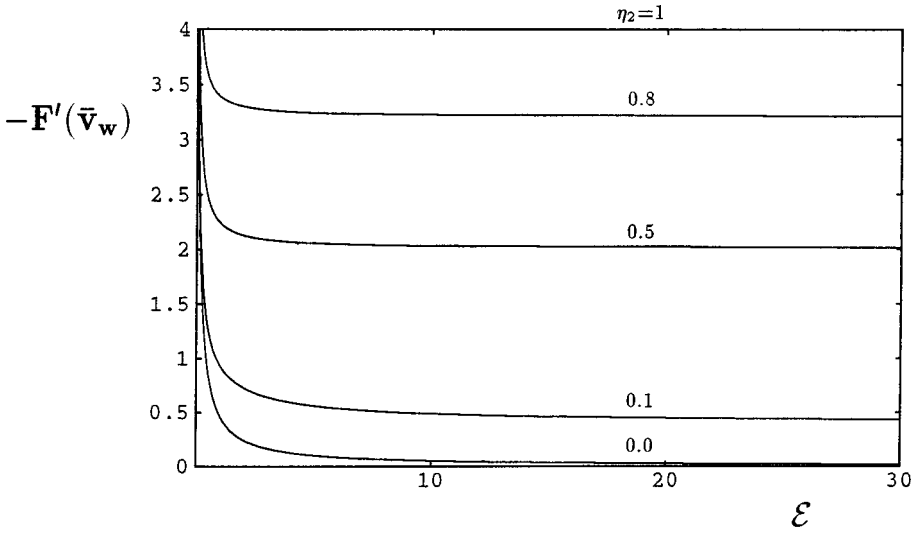

FIG. 3. Neutral stability curves for the round Poiseuille flow of an Oldroyd-B fluid with slip at the wall and constant volumetric flow rate; solutions above the corresponding curve are unstable.

If $F'(\bar{v}_w) > 0$, the solution is stable, independent of the value of the elasticity number ε. If $F'(\bar{v}_w) < 0$, the solution is unstable for values of $F'(\bar{v}_w)$ above the marginal stability curve. Note that $F'(\bar{v}_w)$ cannot be less than -4 due to our assumption that Q is a monotonic function of v_w in steady state [Equation (17)]. Increasing the value of η_2 reduces the size of the instability regime. Moreover, the Newtonian flow ($\varepsilon = 0$ or $\eta_2 = 1$) is always stable.

If, instead of the volumetric flow rate, the pressure gradient is fixed, a basic solution corresponding to negative $F'(\bar{v}_w)$ is unstable, regardless of the value of elasticity number ε. In such a case, one of the other two stable solutions that correspond to the same pressure gradient is attained, depending on the initial condition.

V. NUMERICAL RESULTS FOR THE ONE-DIMENSIONAL FLOW IN A TUBE

We use standard finite elements in space and a fully implicit (Euler backward difference) scheme in time for the numerical solution of the time-dependent one-dimensional equations. Both v_z and T_1^{rz} are approximated with quadratic (P^2–C^0) basis functions. In all results of this section, we take Re $= 1$, $A_1 = 1$, $A_2 = 20$ and $A_3 = 100$; the value of η_2 is 0.1, unless otherwise stated.

The numerical results are found to agree well with the predictions of the linear stability analysis. If a steady-state solution in the negative-slope regime of the slip equation is perturbed, while the pressure gradient is kept constant, the solution evolves to a steady state on one of the two stable branches. On the other hand, if the volumetric flow rate is fixed in the unstable regime, then self-sustained oscillations of the pressure gradient are observed above a critical value of the elasticity number ε. The calculated instability regimes agree well with those predicted by the linear stability analysis. Let us elaborate on the basic solution for Re $= 1$ and $Q = 0.45$ [$F'(\bar{v}_w) = -1.4$]. The linear stability analysis predicts that the flow is unstable for We larger than 0.4 (Figure 3); our numerical results show that the critical value of We at which instability appears might be a little smaller (~ 0.38) if the magnitude of the initial disturbance is large. In Figure 4, we

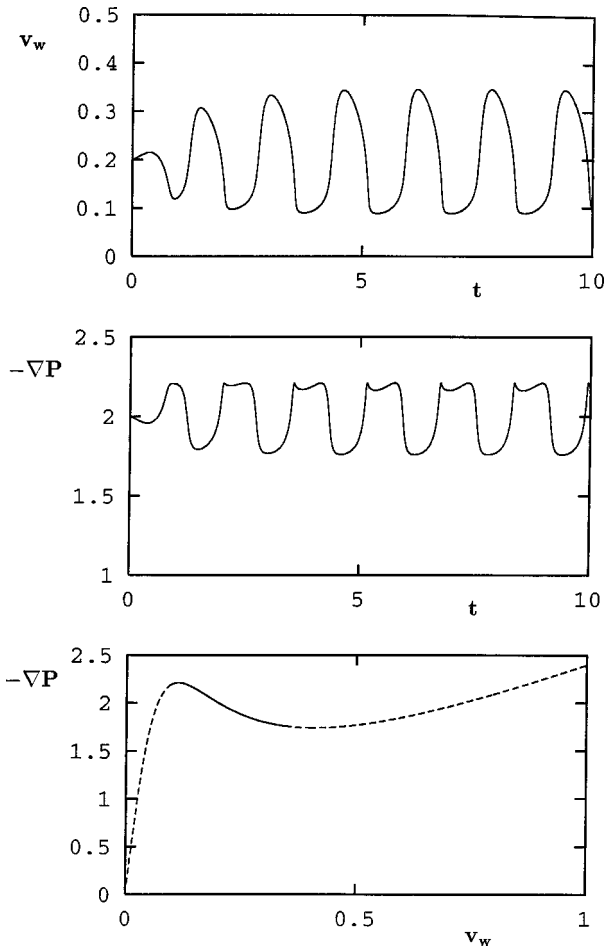

FIG. 4. Evolution of the solution when the unstable steady-state solution for $Q_0 = 0.449$ is perturbed by setting $Q = 0.45$ at $t = 0$; one-dimensional Poiseuille flow, Re = 1, We = 1, and $\eta_2 = 0.1$.

show the evolution of the slip velocity and the pressure gradient when we start from the steady-state solution for We = 1 and $Q_0 = 0.449$ and set $Q = 0.45$ at $t = \Delta t$. The solution becomes periodic after a few oscillations. Note that, in general, the same periodic solution is obtained when Q_0 is much farther from Q, on any of the two positive-slope branches of the slip equation; some exceptions will be discussed toward the end of this section. Indeed, in the sequel, we will preferably show results obtained starting away from the new value of Q, since the periodic solution is more quickly established that way, especially when the Weissenberg number is close to the critical value. In Figure 4(c), we plot the pressure gradient versus the slip velocity as a test for the numerical solution. The plotted quantities move along the steady-state curve as required by Equation (27). The oscillations extend to a small part of the left positive-slope branch of the curve; this results in the appearance of the local minima of the pressure gradient in Figure 4(b). Similarly, local maxima are observed whenever the oscillations extend to the right positive slope branch of the curve.

The effect of We on both the amplitude and the period of the oscillations is illustrated in Figure 5, where we plot the evolution of the slip velocity for various values of We (for

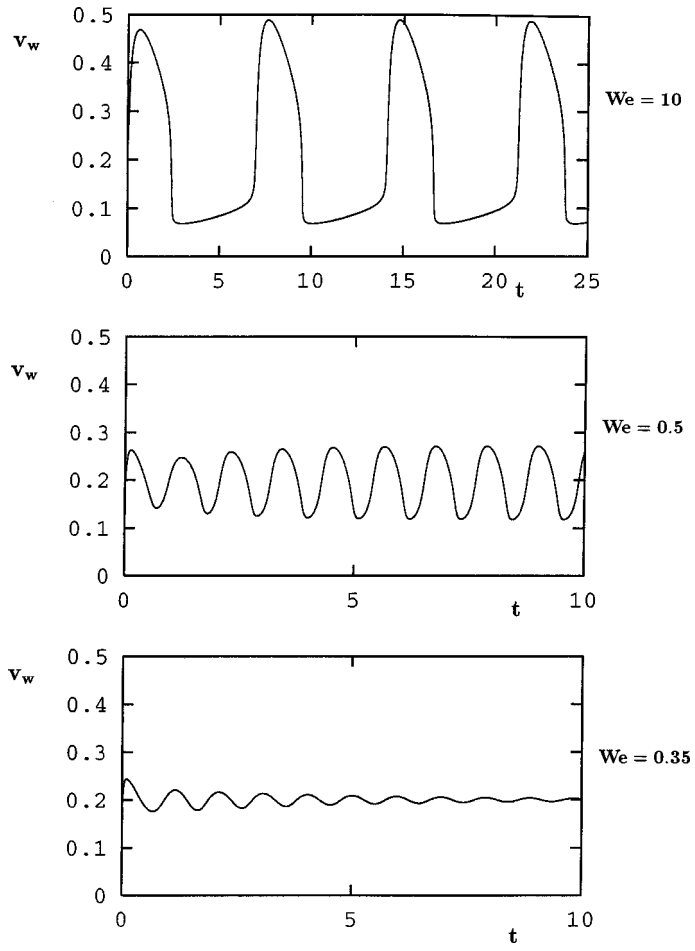

FIG. 5. Time-dependent solutions for different values of We with $Q = 0.45$; one-dimensional Poiseuille flow, Re = 1 and $\eta_2 = 0.1$.

$Q = 0.45$). Both the amplitude and the period of the oscillations decrease as We decreases, and the solution becomes stable below a critical value, in agreement with the linear stability analysis.

The effect of η_2 has also been studied. The steady-state solutions are unstable below a critical value of η_2, in agreement with the linear stability analysis. As the value of η_2 decreases, that is, as we move from the Newtonian to the upper-convected Maxwell model, the flow destabilizes and both the amplitude and the frequency of the oscillations become larger. Finally, the stability of the solutions when $-4\eta_2 < F'(\bar{v}_w) < 0$, i.e., for values of $-F'(\bar{v}_w)$ below the asymptotic limits found at Re $= 0$ has been examined. The calculated responses depend not only on the size of the perturbation, but also on the initial conditions. For small perturbations, the steady-state solution is reached, whereas for relatively larger perturbations, periodic solutions might be obtained.

VI. NUMERICAL RESULTS FOR THE TWO-DIMENSIONAL PROBLEMS

For all results of this section, we take Re $= 1$ and $\eta_2 = 0.1$, unless otherwise stated. The maximum time step Δt_{max} was taken equal to 0.01. The results obtained by taking

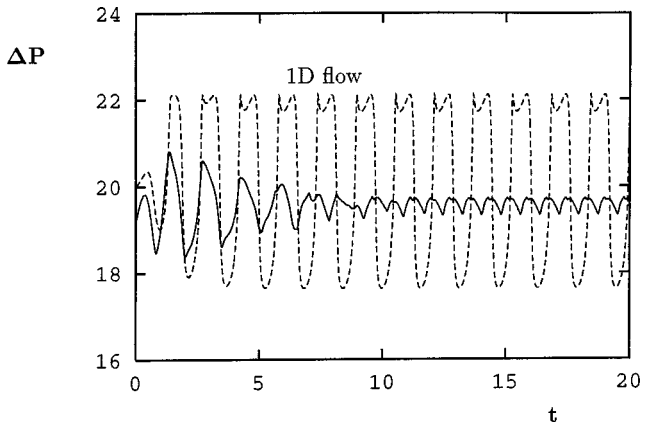

FIG. 6. Evolution of the pressure drop for the two-dimensional circular Poiseuille flow compared to the one-dimensional solution (dashed line); $Q = 0.45$, Re = 1, We = 1 and $L_1 = 10$.

$\Delta t_{max} = 0.001$ were practically the same. Before presenting results for the stick-slip and the extrudate-swell problems, we show results for the two-dimensional Poiseuille flow and compare them to their one-dimensional counterparts.

A. Poiseuille flow

We have first tested our two-dimensional codes by using as inlet boundary conditions the one-dimensional time-dependent solutions calculated in Section V; the other boundary conditions are those given in Section II B. It has been found that, in this case, the one-dimensional solution is convected downstream and, thus, the flow remains one-dimensional at all times, except near the exit. We then obtained results with the velocity at the inlet kept constant. As in Section V, steady-state solutions were perturbed by changing the value of the volumetric flow rate by a small amount (0.1%) at $t = \Delta t$. In all two-dimensional Poiseuille flow calculations, the velocity at the inlet was assumed to be parabolic, following Equation (19). It was found that perturbing an unstable steady state leads again to oscillatory and eventually periodic flow.

In Figure 6, we compare the evolution of the pressure drop for $Q = 0.45$ with its one-dimensional counterpart. The pressure drop ΔP is calculated along the wall and the length of the tube L_1 is taken equal to 10. We observe that the amplitude of the oscillations is much smaller in the two-dimensional case. At early times, the periods of the oscillations are approximately the same. In the two-dimensional flow, however, the period is reduced by almost a half just before periodicity is established. This pattern has been observed in all calculations in which a periodic solution is reached. Note that the initial pressure drops in the one- and the two-dimensional calculations differ, since the disturbed steady-state solution in the two-dimensional case does not correspond to fully developed Poiseuille flow; this is due to the zero normal stress condition used at the exit plane. In fact, due to the rearrangement of the flow at the exit region, the calculated pressure drop along the axis of symmetry is larger than its counterpart along the wall and oscillates with a smaller amplitude.

The most important finding of our two-dimensional calculations is that, when Q is in the unstable regime, the flow is space periodic too. This is clearly seen when plotting the contours of the radial velocity during one cycle. The contour cells of the radial velocity component in Figure 7 are of alternating signs; this implies that the fluid moves periodi-

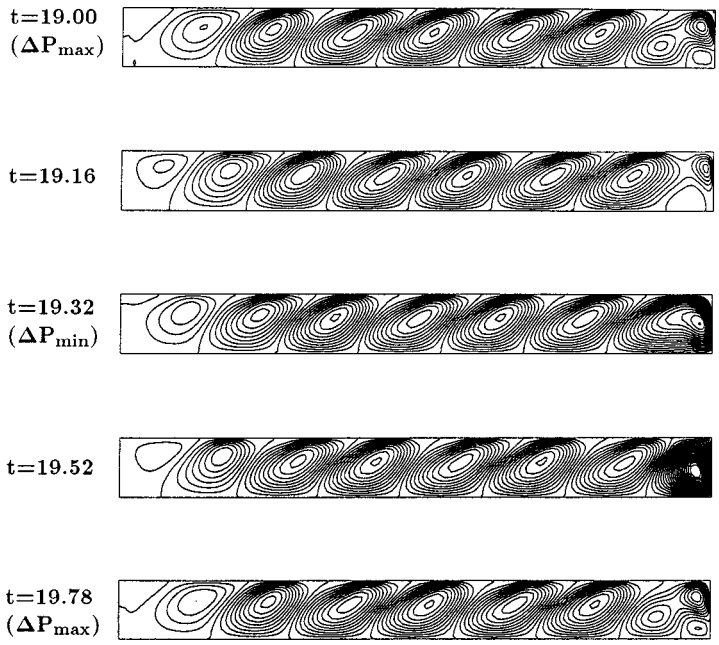

FIG. 7. Contours of the radial velocity in two-dimensional Poiseuille flow during one cycle after periodicity is established; $Q = 0.45$, Re = 1, We = 1 and $L_1 = 10$.

cally from the core towards the wall and vice versa. The fluid accelerates and decelerates periodically in the axial direction. The periodicity in space has been verified by repeating the calculations with a longer mesh. The period of the oscillations and the size of the v_r cells remained the same when we increased L_1 from 10 to 16.

As with the one-dimensional results, the amplitude and the period of the pressure drop oscillations are reduced as the Weissenberg number is decreased, and the flow is stable below a critical value of We. This critical value is higher than the linear stability analysis prediction.

B. Stick-slip and extrudate-swell problems

In this section, we study the effect of the pressure-drop and mass-flow-rate oscillations encountered in Poiseuille flow on the free surface of the extrudate. We also show that the period of the pressure-drop oscillations depends on the boundary conditions at the inlet. We still take $Q = 0.45$, Re = 1, We = 1, and $\eta_2 = 0.1$. The length L_2 of the extrudate is taken equal to 5; in most runs, the length L_1 of the die was taken to be 10. In order to avoid errors caused by the singularity at the exit of the die, we take the pressure drop along the die equal to the value of p at the inlet node of the wall. The calculations confirm the result of Section VI A: when Q is in the unstable regime, the flow in the die is periodic in the axial direction.

The periodic flow in the die generates small-amplitude free surface waves. As with the pressure-drop oscillations, the wavelength of the free surface waves is initially large, while it is considerably reduced once periodicity in time is established (Figure 8). It takes, however, a longer time to reach periodicity with the extrudate-swell and stick-slip flows, since the flow domain is longer. The convergence of the results with mesh refinement has been studied by employing three meshes, the characteristics of which are given

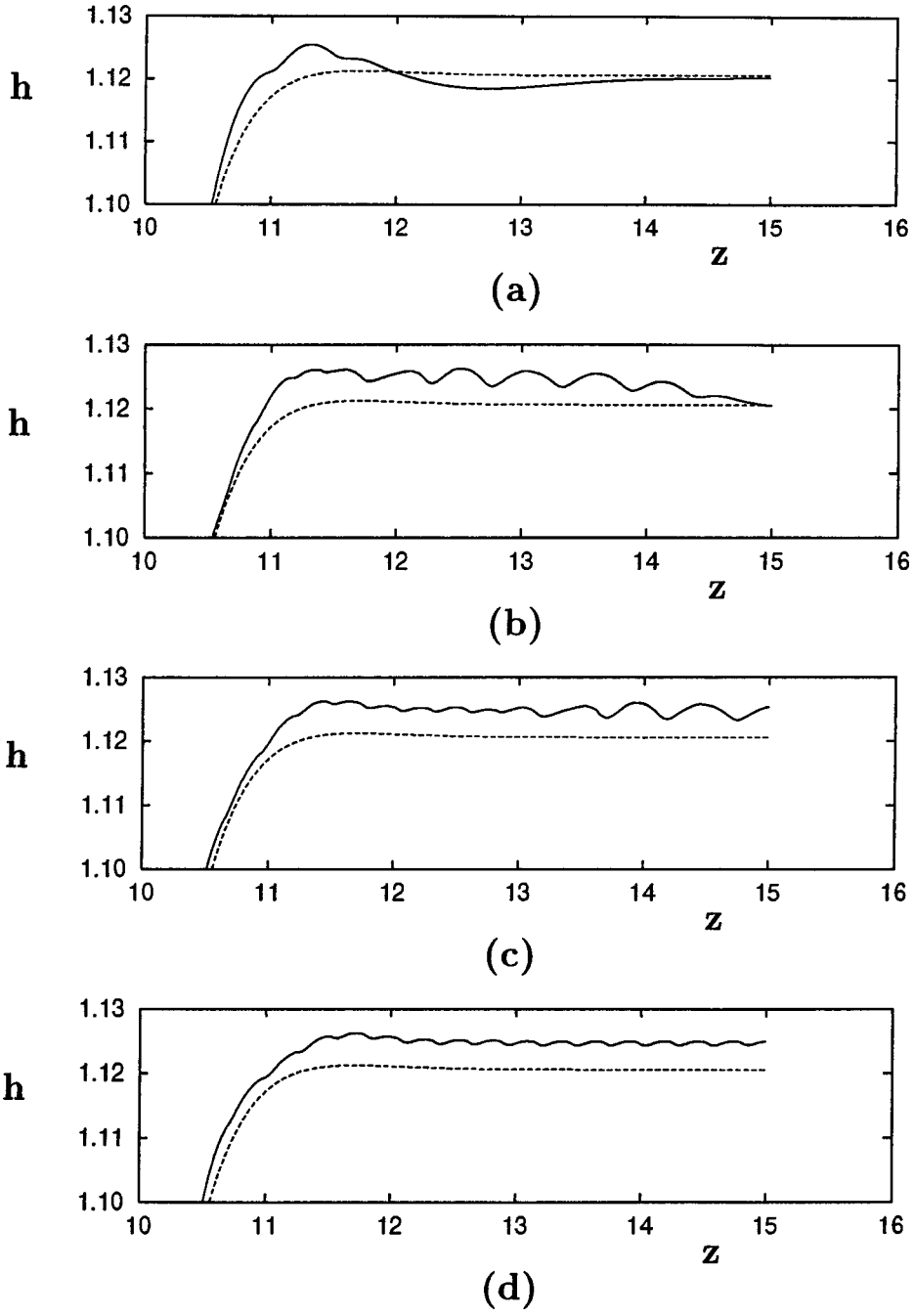

FIG. 8. Detail of the extrudate surface at different times: (a) $t = 6$; (b) $t = 14$; (c) $t = 18$; (d) $t = 25.86$. The last time corresponds to a pressure drop maximum after periodicity is established. The dashed lines show the steady-state solution; the velocity at the inlet is parabolic, $Q = 0.45$, Re $= 1$, We $= 1$ and $\eta_2 = 0.1$.

in Table I. In Table I, we also depict the corresponding wavelengths of the free surface and the periods of the pressure drop. The mean wavelengths are calculated in the z interval (12,14) and at a pressure drop maximum. The convergence of the free surface with mesh refinement has not been pursued any further due to the excessive requirements

TABLE I. Mean wavelength of the free surface and period T_p of the pressure drop obtained with three meshes. The mean wavelengths are calculated in the z interval (12,14) and at a pressure drop maximum. The velocity at the inlet is parabolic, $Q = 0.45$, Re = 1, We = 1 and $\eta_2 = 0.1$.

Mesh	Elements in the die	Elements in the extrudate	Wavelength	T_p
1	54×6	65×6	0.281	0.76
2	54×6	120×6	0.277	0.76
3	120×8	240×8	0.274	0.77

in computational time. In Figure 8(d), we plot a detail of the oscillating free surface at a pressure drop maximum, after periodic flow is established. Since the free-surface waves appear together with pressure-drop oscillations, the proposed mechanism of instability may be related only to the stick-slip extrusion instability and not to sharkskin. In Figure 9, we show the contours of the radial velocity component during one cycle. These results have been obtained by imposing a parabolic velocity profile at the inlet, as given by Equation (19). The frequency of the free surface waves is the same as that of the pressure drop. Indeed, if one multiplies the average velocity of the extrudate (0.356) by the period $T_p = 0.77$ of the pressure drop, one gets the value 0.274 for the wavelength, which coincides with the calculated value in Table I. The velocity cells of Figure 9 are generated at the same frequency as the pressure-drop oscillations; their speed of propagation is more than seven times faster than the average velocity of the fluid in the die.

Finally, in order to investigate the effect of the boundary condition at the inlet on the period of the pressure-drop oscillations, we solved the time-dependent stick-slip problem by imposing parabolic and uniform axial velocity profiles, according to Equations (19) and (21), respectively. Calculated values for the period are tabulated in Table II, along with values obtained for the Poiseuille and extrudate-swell flows under the same flow conditions. We remark that the period of the pressure-drop oscillations is larger when the

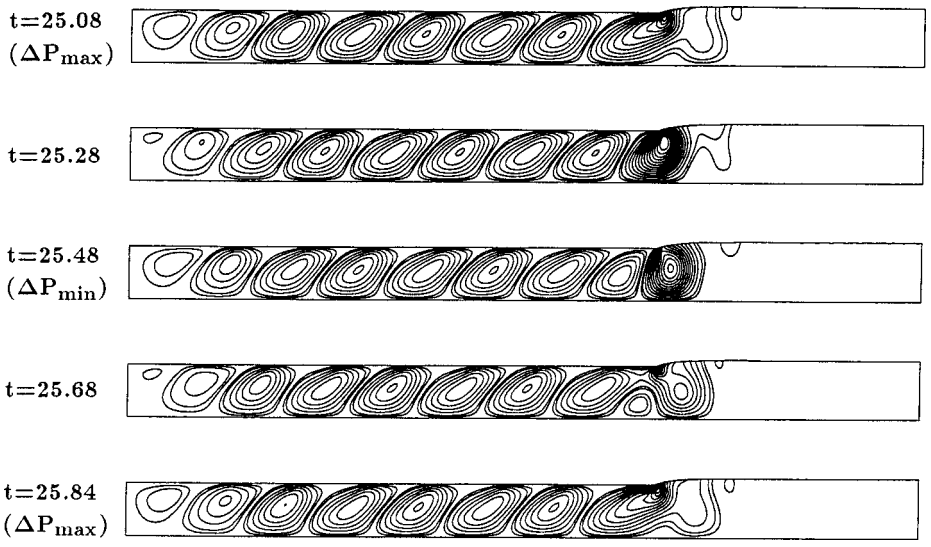

FIG. 9. Contours of the radial velocity in extrudate swell flow during a cycle after periodicity is established; the velocity at the inlet is parabolic, $Q = 0.45$, Re = 1, We = 1 and $\eta_2 = 0.1$.

TABLE II. Effect of the inlet boundary condition on the period T_p of the pressure-drop oscillations; $Q = 0.45$, Re = 1, We = 1 and $\eta_2 = 0.1$.

Flow	v_z at the inlet	L_1	T_p
Poiseuille	parabolic	10	0.78
extrudate-swell	parabolic	10	0.77
stick-slip	parabolic	10	0.78
stick-slip	plug	10	0.90
stick-slip	plug	15	0.91

velocity at the inlet is uniform. The contours of the radial velocity component during one cycle are shown in Figure 10. Since the period is larger, the contour cells are larger than those in Figure 9. Runs with longer meshes revealed that the period of the oscillations does not depend on the length of the die (see Table II).

VII. CONCLUSIONS

A mechanism for extrusion instability that does not require any multiplicities of the stress constitutive equation has been proposed. We have shown that, under certain conditions, the combination of viscoelasticity and nonlinear slip at the wall of the die leads to self-sustained oscillations of the pressure drop similar to those observed experimentally in the stick-slip instability regime.

We first studied the one-dimensional axisymmetric Poiseuille flow of an Oldroyd-B fluid by means of a one-dimensional linear stability analysis and time-dependent finite element calculations. We demonstrated the existence of unstable solutions in the negative slope regime of the flow curve. The instability regimes grow in size as the Weissenberg number is increased. The incompressible Newtonian flow is always stable; flow destabilizes as one moves towards the upper-convected Maxwell model. If a steady-state solution in the negative-slope regime is perturbed at constant pressure gradient, a stable

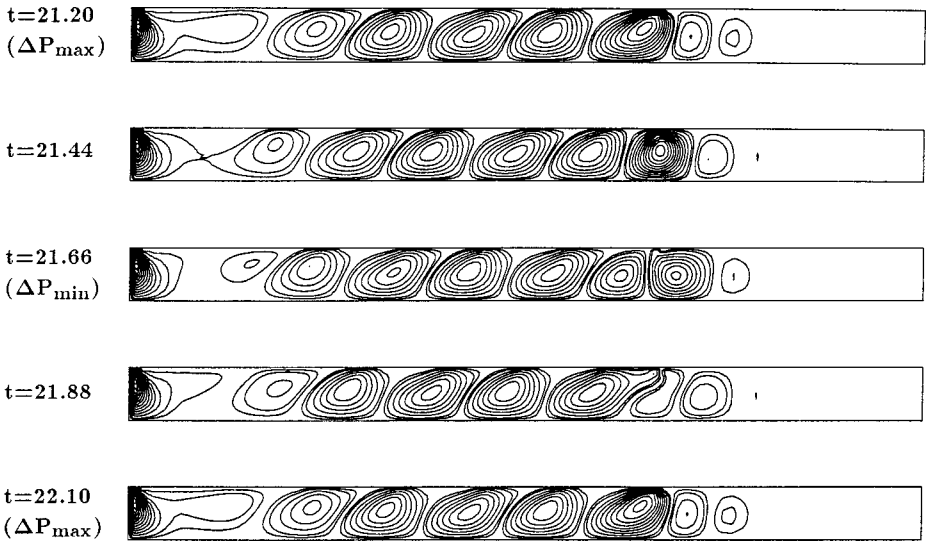

FIG. 10. Contours of the radial velocity in stick-slip flow during a cycle after periodicity is established; the velocity at the inlet is uniform, $Q = 0.45$, Re = 1, We = 1, $\eta_2 = 0.1$, $L_1 = 10$ and $L_2 = 5$.

steady-state solution on one of the two positive-slope branches of the flow curve is eventually reached. If, however, the unstable steady-state solution is perturbed at constant volumetric flow rate, the response is initially oscillatory, while it eventually becomes periodic. The amplitude and the period of the oscillations are increasing functions of the Weissenberg number.

The two-dimensional axisymmetric Poiseuille, stick-slip and extrudate-swell flows of an Oldroyd-B fluid have also been solved using the EVSS method. Periodic solutions are again found to exist in the unstable regime. Nevertheless, the amplitude and the period of the oscillations are smaller than in the one-dimensional flow. A consequence of the deviations from the one-dimensional time-dependent Poiseuille solution is that the flow in the die becomes periodic in the axial direction. Our calculations demonstrate that the period of the pressure-drop oscillations depends on the inlet boundary conditions and that the periodic flow in the die generates small-amplitude waves on the surface of the extrudate.

It should be emphasized that making comparisons with experiments is out of the scope of the present work. Our objective is simply to demonstrate that viscoelasticity combined with nonlinear slip can generate oscillations of the pressure drop in Poiseuille flow, similar to those observed experimentally with the stick-slip extrusion instability, and to show the notable differences between the one- and the two-dimensional calculations. There are many important issues that should be addressed in order to proceed to realistic extrusion instability simulations. A truly representative constitutive equation for polymer fluids under the critical conditions and an accurate slip equation based on polymer/wall adhesion physics should be used. Moreover, a real simulation should take into account the bulk polymer compressibility and the inherent polymer chain flexibility. (Therefore, it is important to include the reservoir region.) Only after considering all the above factors, one can proceed to predictions of the critical conditions for onset of slip and/or unstable flow and study the features of extrudate distortions such as periods, wavelengths, amplitudes and wave patterns.

ACKNOWLEDGMENTS

This paper presents research results of the Belgian Program on Interuniversity Poles of Attraction, initiated by the Belgian State, Prime Minister's Office for Science, Technology and Culture. The scientific responsibility rests with its authors. The authors wish to thank Vincent Navez for performing preliminary two-dimensional calculations showing periodicity in space. E.B. is supported by a F.R.I.A. grant. M.F. is partially supported by the Laboratory of Electronic Structure and Laser, FO.R.T.H., Greece.

References

Adewale, K. P. and A. I. Leonov, ''Modeling spurt and stress oscillations in flows of molten polymers,'' Rheol. Acta **36**, 110–127 (1997).

Bodart, Ch. and M. J. Crochet, ''Time-dependent numerical simulation of viscoelastic flow and stability,'' Theoret. Comput. Fluid Dynamics **5**, 57–75 (1993).

Brown, R. A., M. J. Szady, P. J. Northey, and R. C. Armstrong, ''On the numerical stability of mixed finite-element methods for viscoelastic flows governed by differential constitutive equations,'' Theoret. Comput. Fluid Dynamics **5**, 77–106 (1993).

Chen, Y.-L., R. G. Larson, and S. S. Patel, ''Shear fracture of polystyrene melts and solutions,'' Rheol. Acta **33**, 243–256 (1994).

Crochet, M. J., A. R. Davies, and K. Walters, *Numerical Simulation of non-Newtonian Flow* (Elsevier, New York, 1984).

Debae, F., V. Legat, and M. J. Crochet, ''Practical evaluation of four mixed finite element methods for viscoelastic flow,'' J. Rheol. **38**, 421–442 (1994).

Denn, M. M., ''Surface-induced effects in polymer melt flow,'' in *Theoretical and Applied Rheology*, edited by P. Moldenaers and R. Keunings (Elsevier, New York, 1992), 45–49.

El Kissi, N. and J. M. Piau, ''Ecoulement de fluides polymères enchevêtrés dans un capillaire. Modélisation du glissement macroscopique à la paroi,'' C. R. Acad. Sci. Ser. II: Mec., Phys., Chim. **309**, 7–9 (1989).

Fyrillas, M. M. and G. C. Georgiou, ''Linear stability diagrams for the shear flow of an Oldroyd-B fluid with slip along the fixed wall,'' Rheol. Acta (to be published).

Georgiou, G. C., ''On the stability of the shear flow of a viscoelastic fluid with slip along the fixed wall,'' Rheol. Acta **35**, 39–47 (1996).

Georgiou, G. C. and M. J. Crochet, ''Compressible viscous flow in slits, with slip at the wall,'' J. Rheol. **38**, 639–654 (1994a).

Georgiou, G. C. and M. J. Crochet, ''Time-dependent compressible extrudate-swell problem with slip at the wall,'' J. Rheol. **38**, 1745–1755 (1994b).

Kolkka, R. W., D. S. Malkus, M. G. Hansen, G. R. Ierley, and R. A. Worthing, ''Spurt phenomena of the Johnson-Segalman fluid and related models,'' J. Non-Newtonian Fluid Mech. **29**, 303–335 (1988).

Leonov, A. I., ''On the dependence of friction force on sliding velocity in the theory of adhesive friction of elastomers,'' Wear **141**, 137–145 (1990).

Pearson, J. R. A. and C. J. S. Petrie, ''On the melt-flow instability of extruded polymers,'' Proc. 4th Int. Rheological Congress, 1965, Vol. 3, pp. 265–282.

Rajagopalan, D., R. C. Armstrong, and R. A. Brown, ''Finite element methods for calculation of steady, viscoelastic flow using constitutive equations with a Newtonian viscosity,'' J. Non-Newtonian Fluid Mech. **36**, 159–192 (1990).

Yerushalmi, J., S. Katz, and R. Shinnar, ''The stability of steady shear flows of some viscoelastic fluids,'' Chem. Eng. Sci. **25**, 1891–1902 (1970).